Inter-Layer Potential for Graphene/*h*-BN Heterostructures

Supplementary Information

Itai Leven,[1] Tal Maaravi,[1] Ido Azuri,[2] Leeor Kronik,[2] and Oded Hod[1]

[1] *Department of Physical Chemistry, School of Chemistry, The Raymond and Beverly Sackler Faculty of Exact Sciences and The Sackler Center for Computational Molecular and Materials Science, Tel Aviv University, Tel Aviv 6997801, Israel*

[2] *Department of Materials and Interfaces, Weizmann Institute of Science, Rehovoth 76100, Israel*

Basis Set Superposition Error

As described in the main text the force-field parameterization has been performed using the tier-2 basis set,[1] as implemented in the FHI-AIMS suite of programs,[2] with tight convergence settings. This basis set is known to introduce minor basis set superposition errors (BSSE) in dimer calculations.[3, 4] In order to estimate the BSSE in the present case, we have performed counterpoise (CP)[5, 6] BSSE correction calculations on the borzaine/benzene dimer. Fig. S1 presents binding energy curves of the dimer calculated using the screened-exchange HSE density functional approximation[7-10] with (red) and without (black) CP BSSE correction, the TS-vdW[11] dispersion augmented HSE functional with (blue) and without (green) CP BSSE correction, and the HSE functional with (purple) and without (brown) CP BSSE correction augmented by many-body dispersion (MBD)[12, 13] effects. The CP BSSE energy corrections at the corresponding equilibrium inter-dimer distances are 0.10(-0.22), 0.07(-7.80), and 0.16(-5.54) meV/atom for the HSE, TS-vdW+HSE, and HSE+MBD methods, respectively. Values in the parentheses are the calculated binding energies after the CP BSSE correction. This clearly indicates that BSSE effects are well below the expected force-field fitting accuracy and therefore can be safely neglected.

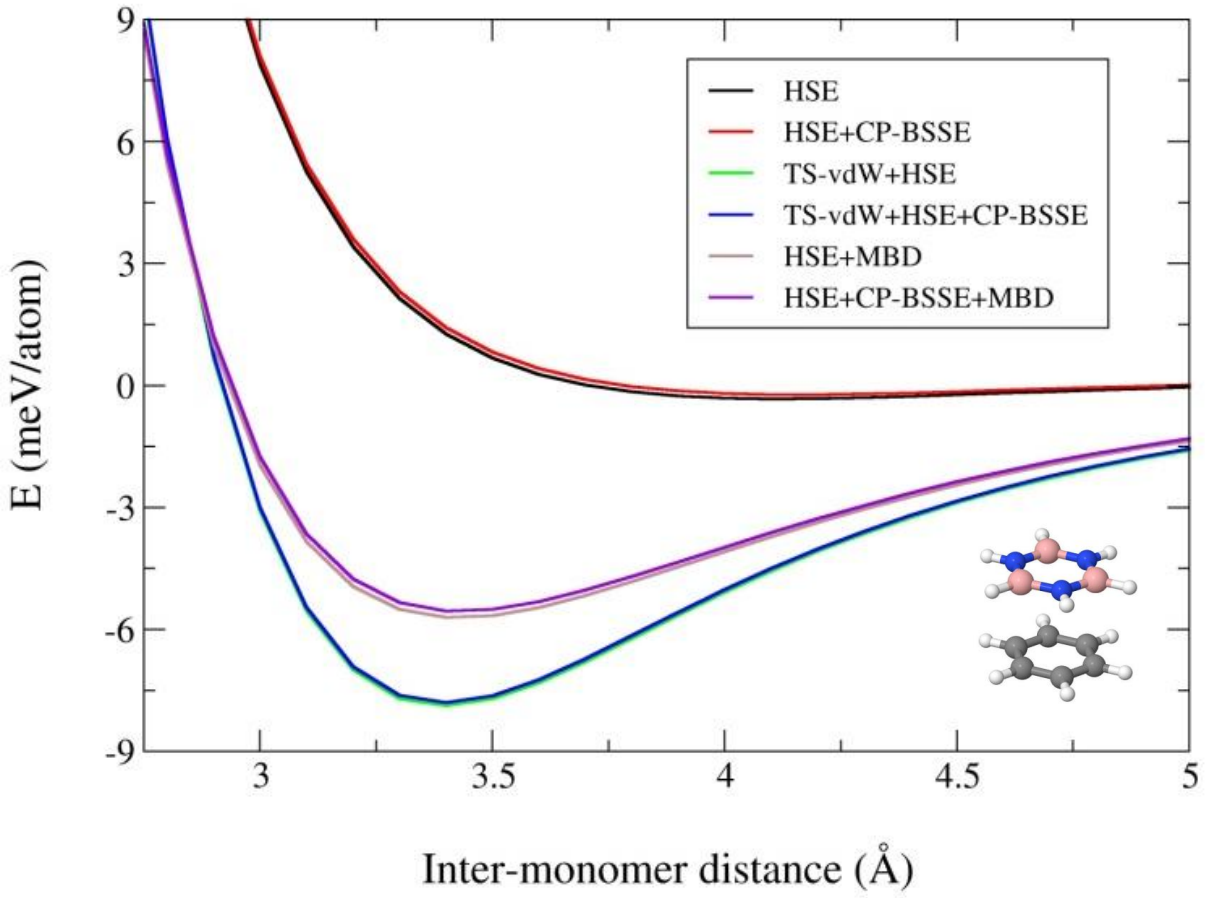

Figure S1: Basis set superposition errors. Binding energy curves of the borzaine/benzne dimer calculated using: (i) the HSE functional with (red) and without (black) CP BSSE correction; (ii) the TS-vdW corrected HSE functional with (blue) and without (green) CP BSSE correction; and (iii) the HSE functional with (purple) and without (brown) CP BSSE correction augmented by many-body dispersion treatment of long-range correlation.

Convergence Settings

As mentioned in the main text we used tight convergence settings throughout our FHI-AIMS calculations. These imply the tightest division of the radial grid, which contains 49, 65, 69, and 71 shells for H, B, C, and N, where the outermost shell is located at distance of 7 Å. The distribution of actual grid points on these shells is done using Lebedev grids,[14] which are designed to integrate all angular momenta up to a certain order, *l*, exactly.[2] The sum of eigenvalues converged to the level of 10^{-3} eV and the volume integrated root-mean square change of the charge density between two consecutive self-consistent field iterations was 10^{-5} electrons. Furthermore, we have converged the self-consistent total energies up to 10^{-6} eV.

Local Registry Index for Graphene/*h*-BN

In this section we briefly summarize the basic principles of the local registry index (LRI) method used in the main text to characterize the registry patterns of the periodic bilayer of graphene/*h*-BN. A detailed description of the method can be found in Ref. 15.

The LRI is a tool developed to characterize the *local* degree of lattice commensurability between adjacent layers. It is based on the global registry index (GRI) approach that quantifies the *overall* inter-lattice registry at various stacking configurations of rigid interfaces.[16] In general terms, the LRI is defined as the average GRI of the local environment of a given atom on one surface, with all atoms of its adjacent surface. To this end, each atom is given a number ranging from 0 (optimal registry) to 1 (worst registry) that quantifies its local registry. Here, optimal and worst stand for the energetically most and least favorable local stacking modes, respectively (see Fig. S2).

Similar to the GRI, the LRI is evaluated via the calculation of projected overlaps between circles assigned to atoms on adjacent layers. For flat surfaces the projected circle overlap area of atoms *i* and *n* located on adjacent layers, $S(\rho_{in})$, is a simple function of their lateral distance, ρ_{in}, which, in turn, is taken as the distance between atom *n* and the surface normal of atom *i*. The latter is defined as the normal to the plane formed by the three nearest neighbors of atom *i*.[3] Unlike the case of flat surfaces, for curved systems $\rho_{in} \neq \rho_{ni}$ and therefore the circle overlap is

taken as the average $S_{in} = 0.5 \cdot [S(\rho_{in}) + S(\rho_{ni})]$, which reduces to $S(\rho_{in})$ for flat surfaces where $\rho_{in} = \rho_{ni}$.

With this, the LRI of a given atom, *i*, on the graphene layer within the heterogeneous graphene/h-BN interface is defined as:

$$LRI_{Graphene/h-BN} = \frac{1}{3}\sum_{n=j,k,l} \frac{\left[\left(S_i^{CN} + S_n^{CN}\right) - \left(S_i^{CN,Opt} + S_n^{CN,Opt}\right)\right] + \left[\left(S_i^{CB} + S_n^{CB}\right) - \left(S_i^{CB,Opt} + S_n^{CB,Opt}\right)\right]}{\left[\left(S_i^{CN,Worst} + S_n^{CN,Worst}\right) - \left(S_i^{CN,Opt} + S_n^{CN,Opt}\right)\right] + \left[\left(S_i^{CB,Worst} + S_n^{CB,Worst}\right) - \left(S_i^{CB,Opt} + S_n^{CB,Opt}\right)\right]},$$

where the sum is taken over the three nearest neighbors (*j*, *k*, and *l*) of atom *i*, and $S_m^{CM,Opt}$, $S_m^{CM,Worst}$, and S_m^{CM} are the sum of pair overlaps of the circle associated with a carbon atom *m* on the graphene layer and all circles of type *M* (B or N) on the adjacent layer obtained at the optimal, worst, and a general local stacking mode, respectively. A similar definition holds for the LRI of the B and N atoms within the *h*-BN layer. For the LRI calculations presented in the main text we adopt the circle radii of the graphene/*h*-BN system suggested in Ref. 17 where $r_C = 0.5a_{CC}$, $r_B = 0.2a_{BN}$, and $r_N = 0.4a_{BN}$, with $a_{CC} = 1.42$ Å and $a_{BN} = 1.446$ Å being the C-C and B-N intralayer covalent bond lengths, respectively.

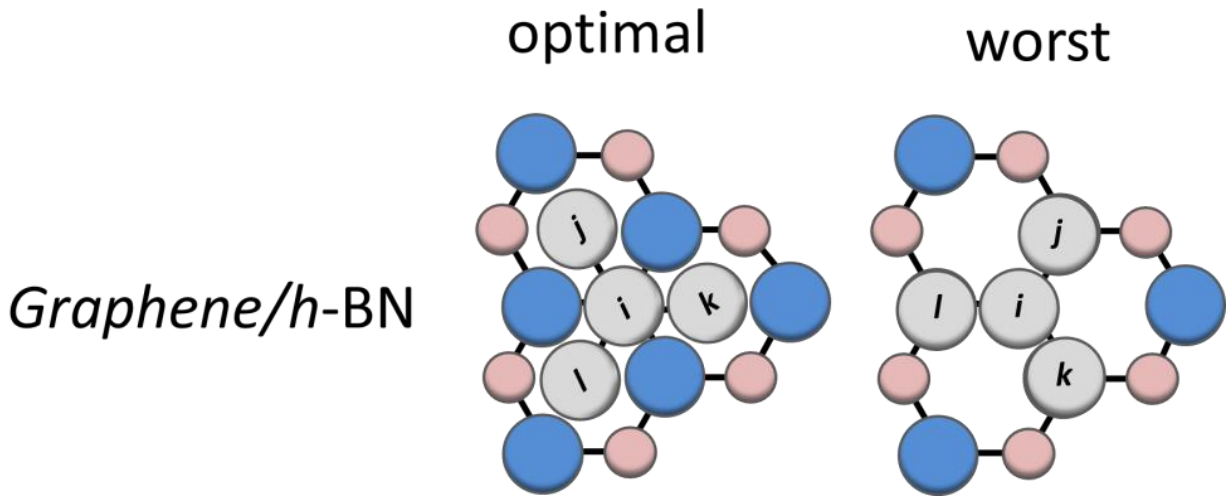

Figure S2: LRI optimal and worst stacking configurations. Schematic representation of the optimal (left) and worst (right) local stacking configurations of atom *i* and its three nearest neighbors *j*, *k* and *l* in the heterogeneous graphene/*h*-BN system. Pink, grey, and blue circles represent boron, carbon, and nitrogen atoms, respectively.

References

1. Havu, V.; Blum, V.; Havu, P.; Scheffler, M., Efficient O(N) integration for all-electron electronic structure calculation using numeric basis functions. *J. Comput. Phys.* 2009, 228, 8367-8379.
2. Blum, V.; Gehrke, R.; Hanke, F.; Havu, P.; Havu, V.; Ren, X. G.; Reuter, K.; Scheffler, M., Ab initio molecular simulations with numeric atom-centered orbitals. *Comput. Phys. Commun.* 2009, 180, 2175-2196.
3. Leven, I.; Azuri, I.; Kronik, L.; Hod, O., Inter-Layer Potential for Hexagonal Boron Nitride. *J. Chem. Phys.* 2014, 140, 104106.
4. Marom, N.; Tkatchenko, A.; Scheffler, M.; Kronik, L., Describing Both Dispersion Interactions and Electronic Structure Using Density Functional Theory: The Case of Metal–Phthalocyanine Dimers. *J. Chem. Theory Comput.* 2010, 6, 81-90.
5. Boys, S. F.; Bernardi, F., The Calculation of Small Molecular Interactions by the Differences of Separate Total Energies. Some Procedures with Reduced Errors. *Mol. Phys.* 2002, 100, 65-73.
6. Simon, S.; Duran, M.; Dannenberg, J. J., How Does Basis Set Superposition Error Change the Potential Surfaces for Hydrogen-Bonded Dimers? *J Chem Phys* 1996, 105, 11024-11031.
7. Heyd, J.; Scuseria, G. E.; Ernzerhof, M., Hybrid functionals based on a screened Coulomb potential. *J. Chem. Phys.* 2003, 118, 8207-8215.
8. Heyd, J.; Scuseria, G. E., Assessment and validation of a screened Coulomb hybrid density functional. *J. Chem. Phys.* 2004, 120, 7274-7280.
9. Heyd, J.; Scuseria, G. E., Efficient hybrid density functional calculations in solids: Assessment of the Heyd-Scuseria-Ernzerhof screened Coulomb hybrid functional. *J. Chem. Phys.* 2004, 121, 1187-1192.
10. Heyd, J.; Scuseria, G. E.; Ernzerhof, M., Erratum: ``Hybrid functionals based on a screened Coulomb potential'' [J. Chem. Phys. 118, 8207 (2003)]. *J. Chem. Phys.* 2006, 124, 219906-1.
11. Tkatchenko, A.; Scheffler, M., Accurate Molecular Van Der Waals Interactions from Ground-State Electron Density and Free-Atom Reference Data. *Phys. Rev. Lett.* 2009, 102, 073005.
12. Tkatchenko, A.; DiStasio, R. A.; Car, R.; Scheffler, M., Accurate and Efficient Method for Many-Body van der Waals Interactions. *Phys. Rev. Lett.* 2012, 108, 236402.
13. Ambrosetti, A.; Reilly, A. M.; DiStasio, R. A.; Tkatchenko, A., Long-Range Correlation Energy Calculated from Coupled Atomic Response Functions. *J. Chem. Phys.* 2014, 140, 18A508.
14. Lebedev, V. I.; Laikov, D. N., A quadrature formula for the sphere of the 131st algebraic order of accuracy. *Dokl. Math.* 1999, 59, 477–481.
15. Leven, I.; Guerra, R.; Vanossi, A.; Tosatti, E.; Hod, O., Multi-Walled Nanotube Faceting Unravelled. *Submitted* 2016.
16. Hod, O., Quantifying the Stacking Registry Matching in Layered Materials. *Isr. J. Chem.* 2010, 50, 506-514.
17. Leven, I.; Krepel, D.; Shemesh, O.; Hod, O., Robust Superlubricity in Graphene/h-BN Heterojunctions. *J. Phys. Chem. Lett.* 2013, 4, 115-120.